Appl. Math. Mech. -Engl. Ed., **39**(3), 365–378 (2018)

Applied Mathematics and Mechanics (English Edition)

https://doi.org/10.1007/s10483-018-2308-9

A new nonlinear force model to replace the Hertzian contact model in a rigid-rotor ball bearing system*

Yulin JIN[1], Zhenyong LU[1], Rui YANG[1], Lei HOU[1,2,†], Yushu CHEN[1]

1. School of Astronautics, Harbin Institute of Technology, Harbin 150001, China;
2. School of Energy Science and Engineering, Harbin Institute of Technology, Harbin 150001, China

(Received Jul. 20, 2017 / Revised Sept. 6, 2017)

Abstract A new nonlinear force model based on experimental data is proposed to replace the classical Hertzian contact model to solve the fractional index nonlinearity in a ball bearing system. Firstly, the radial force and the radial deformation are measured by statics experiments, and the data are fitted respectively by using the Hertzian contact model and the cubic polynomial model. Then, the two models are compared with the approximation formula appearing in Aeroengine Design Manual. In consequence, the two models are equivalent in an allowable deformation range. After that, the relationship of contact force and contact deformation for single rolling element between the races is calculated based on statics equilibrium to obtain the two kinds of nonlinear dynamic models in a rigid-rotor ball bearing system. Finally, the displacement response and frequency spectrum for the two system models are compared quantitatively at different rotational speeds, and then the structures of frequency-amplitude curves over a wide speed range are compared qualitatively under different levels of radial clearance, amplitude of excitation, and mass of supporting rotor. The results demonstrate that the cubic polynomial model can take place of the Hertzian contact model in a range of deformation.

Key words rolling element bearing, Hertzian contact, fractional index, cubic polynomial, rotor ball bearing system

Chinese Library Classification O32
2010 Mathematics Subject Classification 74H45

1 Introduction

Advanced turbomachinery will be presenting higher performance and machinery efficiency under the high rotational speed condition, and the performance and working stability of ball bearings have become increasingly important[1–8]. However, the rotor-rolling element bearings

* Citation: Jin, Y. L., Lu, Z. Y., Yang, R., Hou, L., and Chen, Y. S. A new nonlinear force model to replace the Hertzian contact model in a rigid-rotor ball bearing system. *Applied Mathematics and Mechanics* (*English Edition*), **39**(3), 365–378 (2018) https://doi.org/10.1007/s10483-018-2308-9

† Corresponding author, E-mail: houlei@hit.edu.cn

Project supported by the National Basic Research Program (973 Program) of China (No. 2015CB057400), the National Natural Science Foundation of China (No. 11602070), the China Postdoctoral Science Foundation (No. 2016M590277), and the Heilongjiang Postdoctoral Financial Assistance (No. LBH-Z16067)

©Shanghai University and Springer-Verlag GmbH Germany, part of Springer Nature 2018

system is an intrinsic nonlinear system. The Hertzian analytical formulation of contact force and contact deformation between the balls and races present the fractional index nonlinearity[1–33], and it is coupled with other sources of nonlinearity, such as radial clearance, varying compliance (VC), surface waviness or surface defect, leading to very complex dynamic behaviors of the rotor ball bearing system. As a consequence, the traditional nonlinear methods such as the averaging method, the asymptotic method, the multi-scale method, the Chen-Langford (C-L) method, and the singularity theory are unable to solve this problem analytically.

To investigate the nonlinear dynamical problems of a rolling element bearings system, consequently, it mainly depended on numerical analysis methods and experimental approaches in the past few decades[10–21]. Sunnersjö[10] proposed a dynamic model that took into account the inertial force, radial clearance, and rotational speed. His results showed that the VC vibration levels of the cylindrical roller bearings depend mainly on the inertial force and rotational speed. Fukata et al.[11] presented a nonlinear rigid rotor-ball bearing model with two degrees of freedom that was subjected to a constant radial load. Their results showed that the rotational speed makes significant influence on the nonlinear behaviors of the system, and the vibration responses may generate beating, chaos-like, super-harmonic, and sub-harmonic motions nearby critical speeds. Two different routes to creating the chaotic motions for nonlinear vibration responses of the rolling element bearing were studied by Mevel and Guyader[12–13] via numerical procedure and experimental strategy. Tiwari and Gupta[14] and Harsha[16–17] investigated nonlinear dynamic responses of a balanced rigid rotor supported by the rolling element bearings with different radial internal clearances and varying rotational speeds. The nonlinear dynamic responses of an unbalanced rigid rotor-bearing system were also studied by Tiwari et al.[15] and Harsha[18]. The effects of the preload and number of balls on the radial and axial vibrations of a rigid rotor-ball bearing system were discussed by Aktürk et al.[19]. By taking into consideration the rolling element centrifugal load, angular contacts, and axial dynamics, Liew et al.[20] established a more comprehensive rotor-bearing dynamic model and designed a test rig to estimate the effect of the rolling element centrifugal load. Jang and Jeong[21–22] presented a nonlinear model of a rigid rotor supported by two or more ball hearings and discussed the effects of the waviness on the nonlinear dynamic responses of the system.

In recent years, the nonlinear dynamic characteristics of rolling element bearing systems have been continually studied. Ghafari et al.[23] investigated the bifurcation of the equilibrium point for a fault-free ball bearing system considering a mass-damper-spring model with the Hertzian contact theory. Bai et al.[24] explored the 1/2 sub-harmonic resonance characteristics of a flexible rotor system supported by ball bearings theoretically and experimentally. Zhang et al.[25–26] presented a comprehensive dynamic model of rotor-bearing system, and the stability was studied by the discrete state transition matrix method. Gunduz and Singh[27] proposed a formulation to evaluate the stiffness of the double row angular contact ball bearings, which was validated by experimental results as well. Nonato and Cavalca[28] developed an elastohydrodynamic (EHD) film point contact model of a deep groove ball bearing to investigate the effects of the lubricant film on the dynamic response of a lumped parameter rotor-bearing system. Xu and Li[29] and Xu[30] investigated the dynamic load and impact response of a planar multi-body system with ball bearing joint. Razpotnik et al.[31] proposed a new method to calculate the bearing stiffness of statically over determined gearboxes. Hou et al.[32] studied the sub-harmonic resonance of a rotor-ball bearing system of aero-engine taking into account the maneuver load. Numerical simulations of the model suggested that it generates not only the 1/2 sub-harmonic resonance, but may also generate the 1/3 or 1/4 sub-harmonic resonance as well. Zhao et al.[33] analyzed the load bearing properties and coefficient of friction of the high speed angular-contact ball bearing. Jin et al.[34] revealed the nonlinear characteristics of VC contact resonance in a rotor-bearing system.

In the above mentioned studies, all the theoretical models of rotor-rolling element bearing system are based on the classical Hertzian contact theory, and as far as we know, almost all

of the literatures and monographs about the nonlinear dynamic problems of bearings widely accepted this theory, because the Hertzian single point contact theory[35–38] is mature and has been testified by experiments. Thus, to use it in ball bearing systems is reasonable, but the fractional index nonlinearity is the thorny problem.

With respect to the above, the present study intends to propose a new model to replace the classical Hertzian contact model. The rest of this paper is organized as follows. In Section 2, the two kinds of nonlinear mechanical models for ball bearing are discussed in statics. Then, in Section 3, the corresponding two types of nonlinear dynamic models for a rigid-rotor ball bearing system are described. In Section 4, the nonlinear dynamic responses of the two models are compared quantitatively and qualitatively. Finally in Section 5, the primary results and conclusions are summarized.

2 Static analysis for two types of nonlinear mechanical models

The experimental rig is shown in Fig. 1. It consists of a rigid rotor-ball bearing system, an AC electric motor, a control system, and a data collection system. The rigid rotor-ball bearing system is simply constructed by a rigid shaft supported by two ball bearings that were the same. A loading device is located at the middle of the rigid rotor-ball bearing system to provide different levels of radial load.

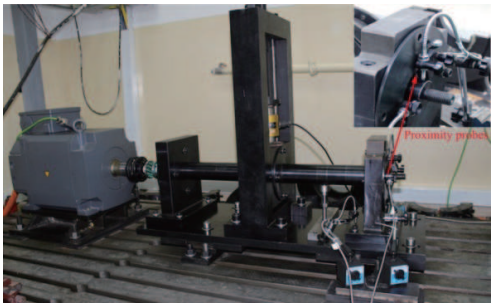

(a) Rigid rotor-ball bearing system

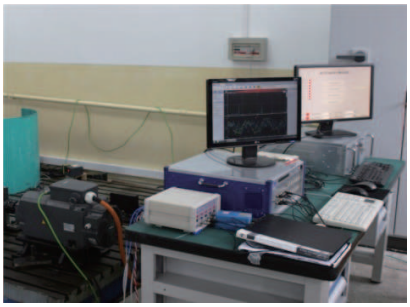

(b) Motor, data collection system

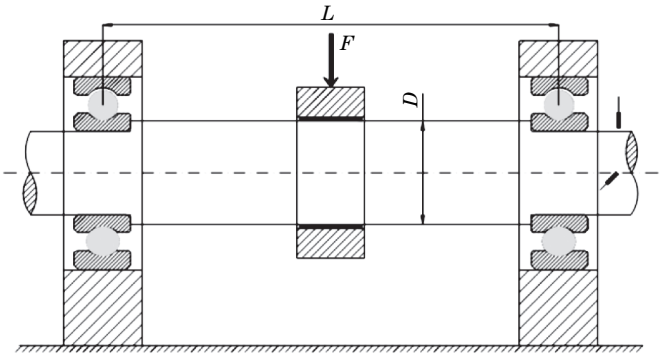

(c) Profile of test rig

Fig. 1 Experimental rig

The geometric parameters of the shaft are as follows: the shaft length $L = 850$ mm and the shaft diameter $D = 65$ mm. In addition, the material parameters of the shaft are as follows: the density $\rho = 7\,950$ kg/m^3, Young's modulus $E = 211$ GPa, and Poisson's ratio $\upsilon = 0.3$. Here,

the shaft is considered as a simply supported beam and the first natural frequency is 808.5 Hz. Therefore, this system can be considered as a rigid rotor-ball bearing system.

The experimental bearing is an SKF6312 deep groove ball bearing, and its parameters are listed in Table 1. The radial contact force and contact deformation in bearing are measured under different levels of radial load by the Bentley high-precision eddy current probes whose resolution is 0.1 μm. In order to reduce the measurement error, two current probes are mounted symmetrically close to the bearing at the right end in the vertical direction, as shown in Fig. 2.

Table 1 SKF6312 ball bearing parameters

Bearing parameter	Value
Number of balls N_b	8
Ball diameter D_b/mm	22.02
Inner raceway diameter d_i/mm	73.62
Outer raceway diameter d_o/mm	117.67
Grade (C_0)[a] clearance/μm	12–36

[a] The American National Standards Institute/American Bearing Manufacturers Association (ANSI/ABMA) Identification Code[1]

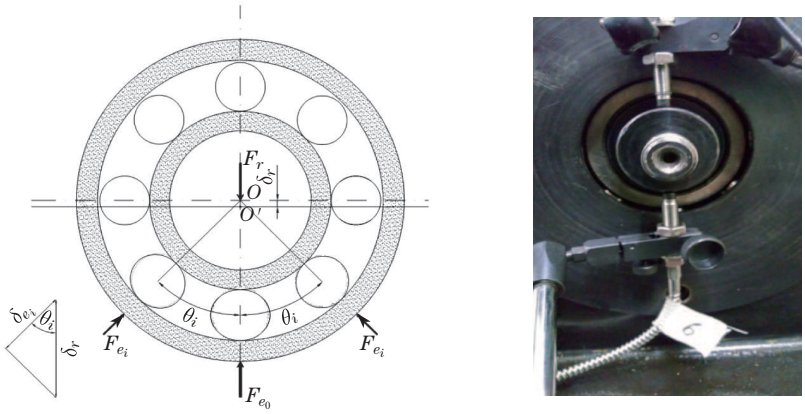

Fig. 2 Radial contact force and contact deformation in bearing

Figure 3 shows the relationships of radial force and radial deformation in a ball bearing which are fitted respectively by using the Hertzian contact formulation and cubic polynomial, and the specific expressions are given as follows:

The Hertzian contact,

$$F_r = C_\mathrm{b}(\delta_r)^{1.5} = 13.26 \times 10^9 (\delta_r)^{1.5} \tag{1}$$

and the cubic polynomial,

$$F_r = a\delta_r^3 + b\delta_r^2 + c\delta_r = -2.38 \times 10^{14}\delta_r^3 + 5.86 \times 10^{11}\delta_r^2 + 6.73 \times 10^7 \delta_r, \tag{2}$$

where F_r represents the radial force (N), δ_r is the radial deformation (m), C_b is the contact stiffness ($\mathrm{N/m^{3/2}}$), and a, b, and c are, respectively, the cubic, quadratic, and linear coefficients of the cubic polynomial. It can be found that the Hertzian analytical formulation is in good agreement with the experimental data when the maximum deformation is under 140 μm, which is not large enough. However, the possibility that these two models are equivalent is in a wide range of deformation. Thus, the predicted maximum deformation value is 1 000 μm based on the experimental Hertzian analytical formulation, and then the data are fitted by cubic polynomial.

As a coincidence, there is an approximation formula about the radial stiffness of ball bearing which appeared in Aeroengine Design Manual[39], given by

$$K_{rr} = 0.117 \times 10^4 \sqrt[3]{F_r n^2 d \cos^5 \beta}, \tag{3}$$

where K_{rr} represents the radial stiffness (N/mm), F_r is the radial force (N), and n, d, and β are the number of contact balls, the ball diameter (mm), and the contact angle, respectively.

The two models are compared with this approximation formula in a wide range of force with the maximum force up to 400 000 N, as shown in Fig. 4. It is clear to see that the Hertzian contact model matches perfectly with the approximation formula, where the maximal error is under 1.1%. The cubic polynomial model also presents a good match for the force less than 300 000 N, and the error is not beyond 2% at 300 000 N. Otherwise, the error will be increased but not beyond 7% at 400 000 N. As a consequence, the two models are approximately equivalent in statics.

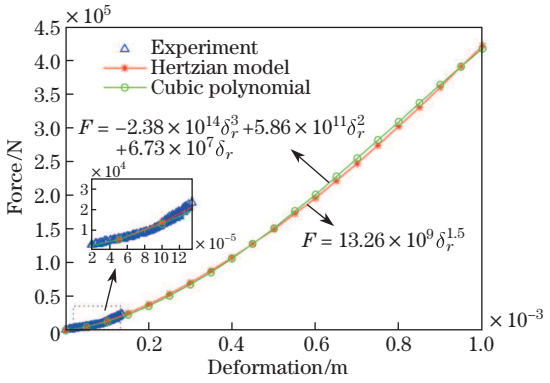

Fig. 3 Experimental data and two kinds of fitted models for radial force and radial deformation

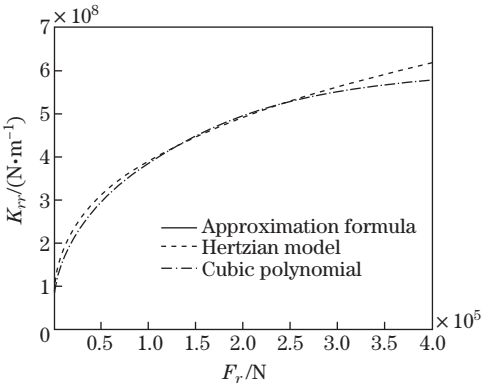

Fig. 4 Comparison between two models and approximation formula for radial stiffness and radial force

The foregoing analysis is mainly the comparison between the Hertzian contact model and the cubic polynomial model for the radial force and radial deformation in bearing. However, the radial force is a resultant force in the vertical direction for the corresponding rolling elements on the loaded area. When the bearing is working, the radial force is varying, but it is assumed that the relationship of contact force and contact deformation between the element and races is a definite formula. For this reason, the two models of relations of contact force and contact deformation for single rolling element between the races are calculated based on statics equilibrium as follows.

The force analysis of the rolling elements in the vertical direction is presented in the first subgraph of Fig. 2. A rolling element is located in the lowest position of outer raceway, marked as '0'. As we know, the roll elements are uniform on the circle with an angle of $2\pi/N_{\mathrm{b}}$. Therefore, the loaded balls are distributed symmetrically on the two sides of that ball. Suppose that each side has k balls, the relations between contact deformation of each rolling element and radial deformation are obtained by geometric analysis[40–41],

$$\delta_{\mathrm{e}}^i = \delta_r \cos(i\theta), \quad i = 0, 1, \cdots, k. \tag{4}$$

Based on the statics equilibrium equation, the radial force is the sum of all the contact forces of the loaded balls which are projected in the vertical direction, and can be written as

$$F_r = F_{\mathrm{e}}^0 + 2\sum_{i=1}^{k} F_{\mathrm{e}}^i \cos(i\theta), \tag{5}$$

where F_{e}^i $(i = 0, 1, \cdots, k)$ are the contact forces of the loaded rolling elements, whose formula depends on the chosen model. For the Hertzian model, $F_{\mathrm{e}} = c_{\mathrm{b}}(\delta_{\mathrm{e}})^{1.5}$, and for the cubic polynomial model, $F_{\mathrm{e}} = a_{\mathrm{e}}\delta_{\mathrm{e}}^3 + b_{\mathrm{e}}\delta_{\mathrm{e}}^2 + c_{\mathrm{e}}\delta_{\mathrm{e}}$. Combining with (4), we thus find that the two models of relations of contact force and contact deformation for a single rolling element are given as follows.

The Hertzian contact model for the single ball is

$$F_{\mathrm{e}} = c_{\mathrm{b}}(\delta_{\mathrm{e}})^{1.5} = 7.20 \times 10^9 (\delta_{\mathrm{e}})^{1.5}. \tag{6}$$

The cubic polynomial model for the single ball is

$$F_{\mathrm{e}} = a_{\mathrm{e}}\delta_{\mathrm{e}}^3 + b_{\mathrm{e}}\delta_{\mathrm{e}}^2 + c_{\mathrm{e}}\delta_{\mathrm{e}} = -1.59 \times 10^{14}\delta_{\mathrm{e}}^3 + 3.43 \times 10^{11}\delta_{\mathrm{e}}^2 + 3.67 \times 10^7 \delta_{\mathrm{e}}. \tag{7}$$

3 Two types of dynamic models in a rigid-rotor ball bearing system

The mechanical model of the rigid rotor-ball bearing system is shown in Fig. 5. It is an ideal model[2–24] of the test rig for theoretically analyzing the nonlinear vibration responses of rotor ball bearing systems. The horizontal rigid shaft is supported by two ball bearings at both ends, the disk is located symmetrically in the middle of the shaft, and the following assumptions[5–8] are made.

(i) There is an interference fit between the shaft and the inner race of the radial ball bearings, and the outer race is fixed to a rigid support.

(ii) It is under a pure rolling condition between the raceway and balls, and the whole system is fault-free.

(iii) The influence between the rolling elements and cage is ignored.

(iv) The inertias of balls introduce little dynamic effect to the system.

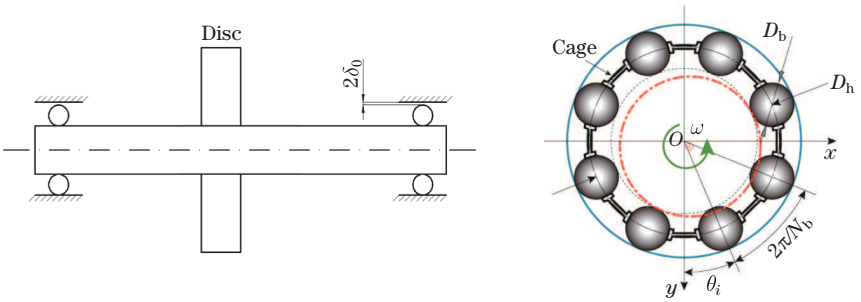

Fig. 5 Sketch map of the rigid-rotor ball bearing system

According to Newton's second law, the differential equations of motions of the rigid-rotor ball bearing model can be formulated as

$$\begin{cases} m\ddot{x} + c\dot{x} + F_x = me\omega^2\cos(\omega t), \\ m\ddot{y} + c\dot{y} + F_y = mg + me\omega^2\sin(\omega t), \\ \begin{Bmatrix} F_x \\ F_y \end{Bmatrix} = \sum\limits_{i=1}^{N} \begin{Bmatrix} F_{\mathrm{e}}(\delta_i)G(\delta_i)\sin\theta_i \\ F_{\mathrm{e}}(\delta_i)G(\delta_i)\cos\theta_i \end{Bmatrix}, \end{cases} \tag{8}$$

where $F_{\mathrm{e}}(\delta_i)$ is the contact force of the ith rolling element. For the classical Hertzian contact model widely used in research applications, the expression is (6), and for the cubic polynomial model proposed in this paper, the formula is (7). Besides,

$$\theta_i = 2\pi(i-1)/N_{\mathrm{b}} + \omega r_{\mathrm{i}} t/(r_{\mathrm{i}} + r_{\mathrm{o}}), \quad \delta_i = x\cos\theta_i + y\sin\theta_i - \delta_0,$$

which are the angular location and contact deformation of the ith rolling element, respectively, and $G(\cdot)$ denotes the Heaviside function, m, c, e, and C_{b} are the mass, damping, offset, and contact stiffness, respectively, ω is the rotational speed, and N_{b}, $2\delta_0$, and r_{i} and r_{o} are the number of balls, the radial clearance, and the inner and outer raceway radii, respectively.

4 Numerical analyses

In order to analyze the similarity of the nonlinear dynamic characteristics for the two models in a rigid-rotor ball bearing system, the displacement responses and frequency spectra of the two models are first compared quantitatively at different rotational speeds by the Runge-Kutta method, and then the structure of frequency-amplitude curves over a wide speed range is compared qualitatively under different levels of radial clearance, magnitude of excitation, and mass of supporting rotor.

Firstly, the quantitative comparisons between the two models are presented. From Fig. 6 to Fig. 8, the stable displacement responses and frequency spectra in the vertical (y) direction and the horizontal (x) direction are depicted at rotational speeds of 300 rad/s, 500 rad/s, and 700 rad/s, and the relative errors of the maximal amplitude of frequency spectrum in both directions between the two models are calculated in Table 2.

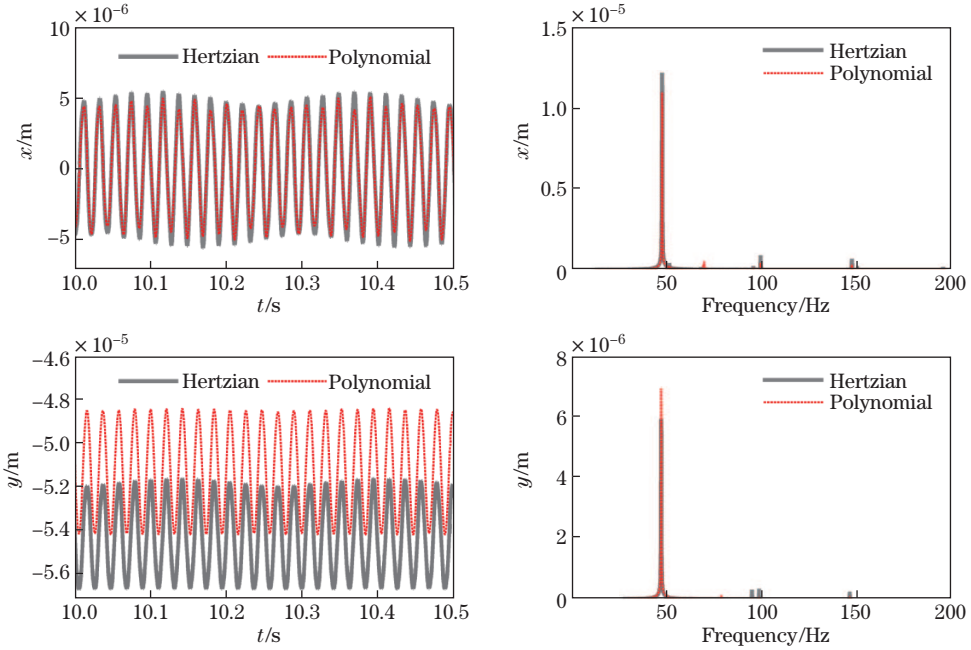

Fig. 6 Displacement responses and frequency spectra in horizontal (x) and vertical (y) directions at speed of 300 rad/s

From Fig. 6 to Fig. 8, it can be seen clearly that the displacement responses and frequency spectra in the horizontal (x) direction for the two models match perfect at each rotational speed, and the relative errors of the maximal amplitude of frequency spectra are less than 10%. In the vertical (y) direction, the corresponding displacement responses present a certain

misalign, because the rotor weight leads to the misalignment of equilibrium positions for the two models in the vertical direction, but the waveforms and frequency spectra still match perfectly, and the maximal amplitude of frequency spectrum is not beyond 11%. As a result, the nonlinear dynamic responses for the two models are quantitatively similar to each other.

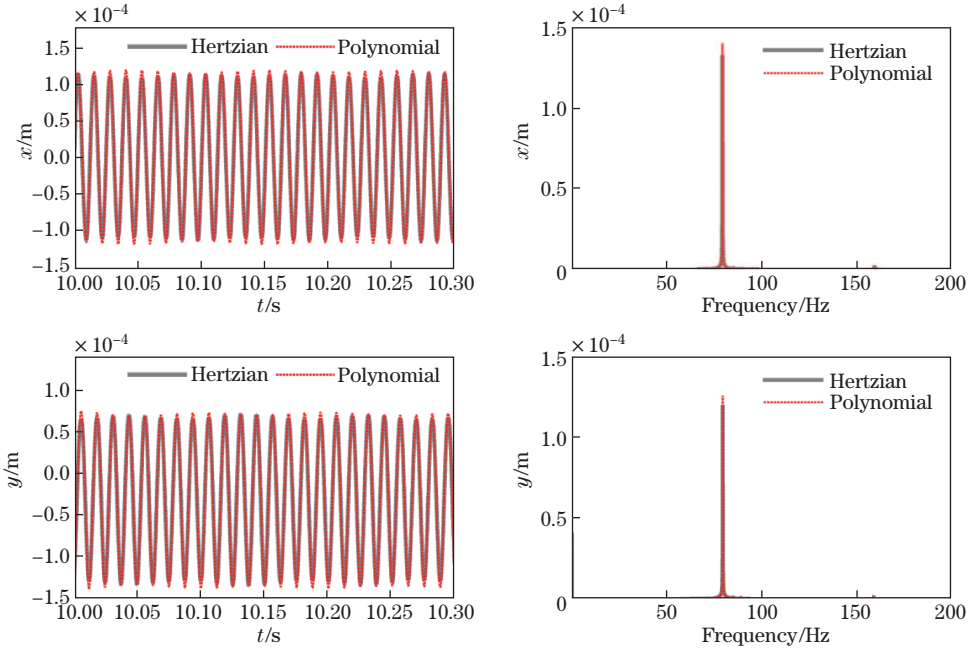

Fig. 7 Displacement responses and frequency spectra in horizontal (x) and vertical (y) directions at speed of 500 rad/s

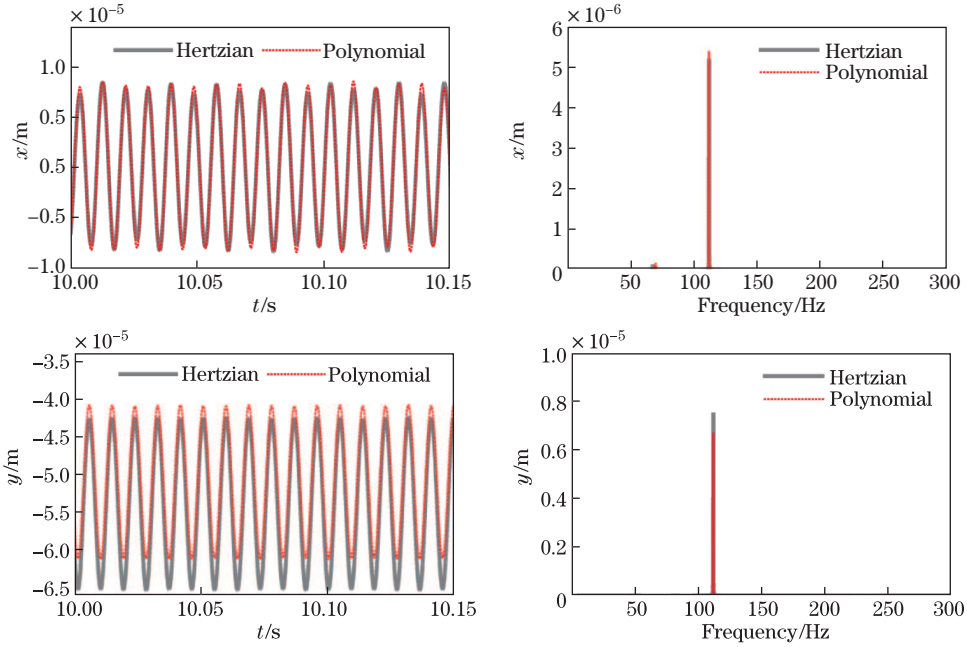

Fig. 8 Displacement responses and frequency spectra in horizontal (x) and vertical (y) directions at speed of 700 rad/s

Nevertheless, the ball bearing system is a complicated nonlinear system, the motion of which is sensitively dependent on initial conditions and parameters. Thus, the nonlinear dynamic behaviors for the two models with different parameters are also compared qualitatively in this section.

Table 2 Relative errors of the maximal amplitude of frequency spectrum

Rotate speed/(rad·s^{-1})	Maximal amplitude/(10^{-6} m)				$\left\lvert\frac{x_h - x_p}{x_h}\right\rvert \times 100\%$	$\left\lvert\frac{y_h - y_p}{y_h}\right\rvert \times 100\%$
	Hertzian		Polynomial			
	x_h	y_h	x_p	y_p		
300	12.280	6.491	11.050	7.003	10.00	7.89
500	13.320	11.980	14.060	12.540	5.56	4.67
700	5.222	7.527	5.413	6.705	3.66	10.92

As shown in Fig. 9, the frequency-amplitude curves for the Hertzian contact model and the cubic polynomial model in the horizontal (x) and vertical (y) directions are plotted with the radial clearances $2\delta_0 = (10, 20, 40, 80)$ μm. It can be found that, for the speed running up and running down, all the frequency-amplitude curves present the hard spring characteristic in both

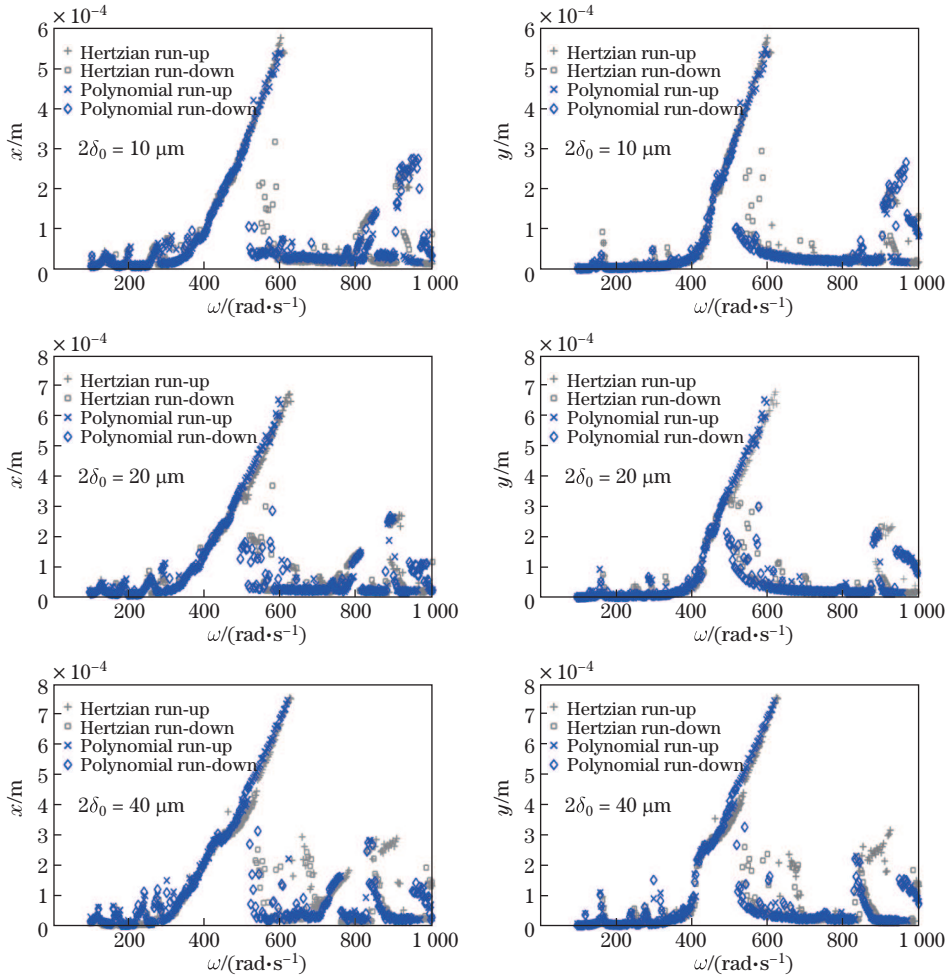

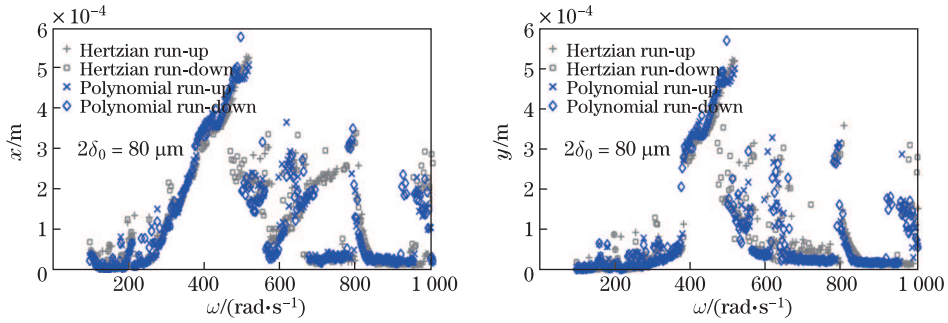

Fig. 9 Frequency-amplitude curves for the two models in horizontal (x) and vertical (y) directions with radial clearances $2\delta_0 = (10, 20, 40, 80)$ μm

directions, and when the radial clearance is less than 40 μm, the frequency-amplitude curves for the two models match perfectly. When the radial clearance is greater than 2×20 μm, the dynamic behaviors are complicated and the frequency-amplitude curves are disheveled for both models, but the structure of the frequency-amplitude curves is very similar.

As shown in Fig. 10, the frequency-amplitude curves for the Hertzian contact model and the cubic polynomial model in the horizontal (x) and vertical (y) directions are depicted with the offset $e = (10, 15, 20, 25)$ μm. It can be found that, for the speed running up and running down, all the frequency-amplitude curves also show the hard spring characteristic in both directions, and with the increase of the offset distance, the dynamic behaviors are complicated too. Nevertheless, all the frequency-amplitude curves for both models still match perfectly.

Finally, it is assumed that the rotor with different mass is supported by the ball bearings. As shown in Fig. 11, the frequency-amplitude curves for the Hertzian contact model and the cubic polynomial model in the horizontal (x) and vertical (y) directions are depicted with the rotor mass of $m = (250, 500, 750, 1\,000)$ kg. It can be found that, for the speed running up and running

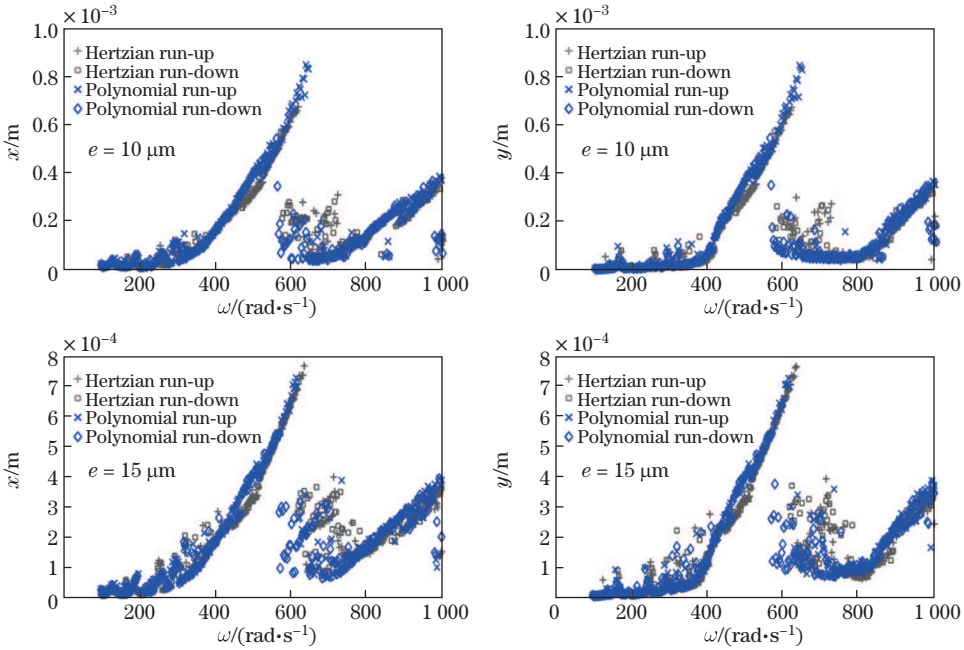

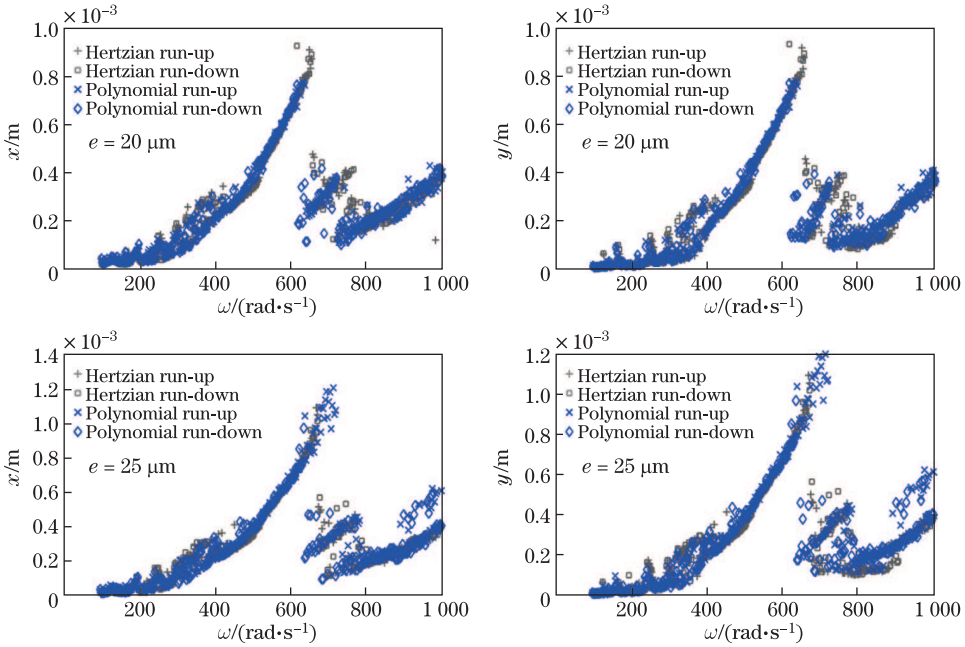

Fig. 10 Frequency-amplitude curves for the two models in horizontal (x) and vertical (y) directions with offset $e = (10, 15, 20, 25)$ μm

down, all the frequency-amplitude curves also show the hard spring characteristic in both directions, and no matter what the rotor mass is, the frequency-amplitude curves for both models present a very good match.

At the end of this part, we can draw a conclusion that the Hertzian contact model and the cubic polynomial model demonstrate almost identical nonlinear dynamic characteristics in the rigid-rotor ball bearing system.

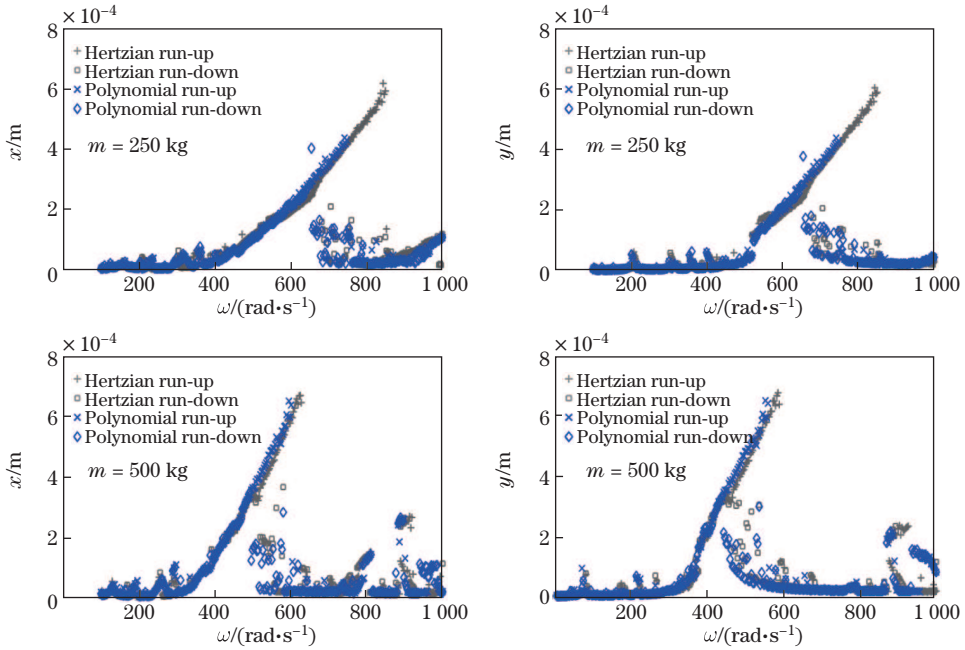

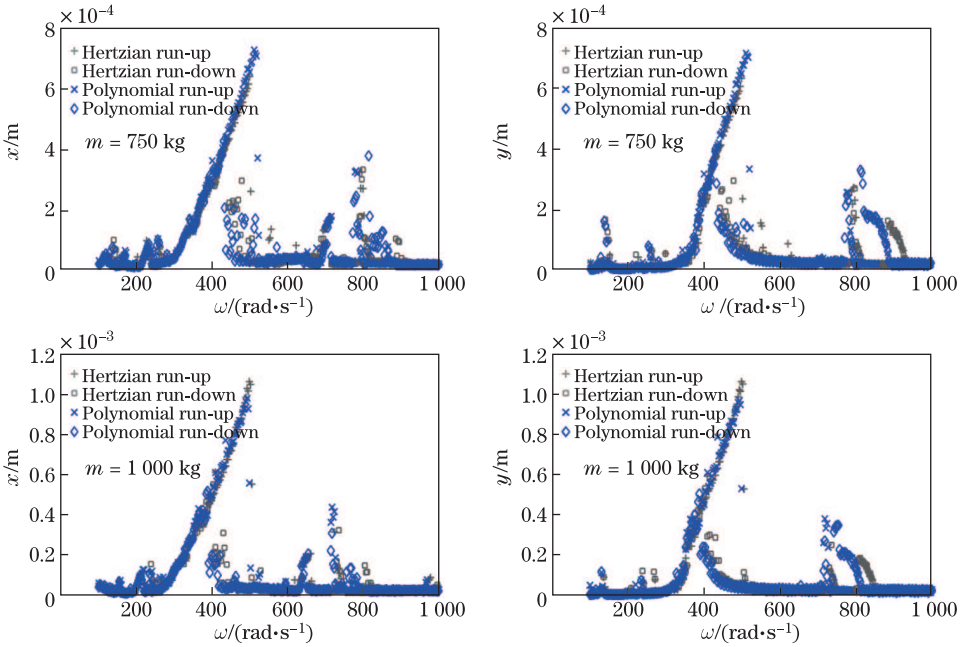

Fig. 11 Frequency-amplitude curves for the two models in horizontal (x) and vertical (y) directions with mass of rotor m=(250, 500, 750, 1 000) kg

5 Conclusions

The Hertzian contact presents the fractional index nonlinearity in a ball bearing system so that the traditional nonlinear methods are unable to solve this problem analytically. In order to solve this thorny problem, this paper proposes a cubic polynomial model to replace the classical Hertzian contact model. The conclusions are summarized as follows.

(i) The radial force and the radial deformation are measured by statics experiments, and the data are fitted by using the Hertzian contact model and cubic polynomial model. Then, the two models are compared with the approximation formula appearing in Aeroengine Design Manual. The maximal error for the Hertzian contact model is under 1.1%, and that for the cubic polynomial model is not beyond 7%. In consequence, the Hertzian contact model and the cubic polynomial model are approximate equivalent in statics.

(ii) The relationship of contact force and contact deformation for single rolling element between the races is calculated based on statics equilibrium, and subsequently the nonlinear dynamic models for the Hertzian contact model and cubic polynomial model in a rigid-rotor ball bearing system are obtained.

(iii) The quantitative comparisons of displacement response and frequency spectrum and the qualitative comparisons of frequency-amplitude curves under different levels of radial clearance, amplitude of excitation, and mass of supporting rotor demonstrate that the nonlinear dynamic characteristics for the Hertzian contact model and cubic polynomial model are almost identical.

Given all this, in all cases considered in this study, the cubic polynomial model can replace the classical Hertzian contact model in a range of deformation so as to investigate the nonlinear dynamic problems of rotor ball bearing system by using traditional nonlinear methods.

Acknowledgements

The authors appreciate for the comments of the editors and reviewers. We appreciate for the support of the China Scholarship Council.

References

[1] Harris, T. A. and Kotzalas, M. N. *Advanced Concepts of Bearing Technology*: *Rolling Bearing Analysis*, 5th ed., Taylor & Francis, London (2006)

[2] Bai, C. Q., Xu, Q. Y., and Zhang, X. L. Nonlinear stability of balanced rotor due to effect of ball bearing internal clearance. *Applied Mathematics and Mechanics* (*English Edition*), **27**(2), 175–186 (2006) https://doi.org/10.1007/s10483-006-0205-1

[3] Hou, L., Chen, Y. S., Fu, Y. Q., Chen, H. Z., Lu, Z. Y., and Liu, Z. S. Application of the HB-AFT method to the primary resonance analysis of a dual-rotor system. *Nonlinear Dynamics*, **88**, 2531–2551 (2017)

[4] Hou, L., Chen, Y. S., Cao, Q. J., and Lu, Z. Y. Nonlinear vibration analysis of a cracked rotor-ball bearing system during flight maneuvers. *Mechanism and Machine Theory*, **105**, 515–528 (2016)

[5] Zhang, Z. Y. *Bifurcations and Hysteresis of Varying Compliance Vibrations of a Ball Bearing-Rotor System*, Ph. D. dissertation, Harbin Institute of Technology (2015)

[6] Zhang, Z. Y. and Chen, Y. S. Harmonic balance method with alternating frequency/time domain technique for nonlinear dynamical system with fractional exponential. *Applied Mathematics and Mechanics* (*English Edition*), **35**(4), 423–436 (2014) https://doi.org/10.1007/s10483-014-1802-9

[7] Zhang, Z. Y., Chen, Y. S., and Li, Z. G. Influencing factors of the dynamic hysteresis in varying compliance vibrations of a ball bearing. *Science China Technological Sciences*, **58**, 775–782 (2015)

[8] Zhang, Z. Y., Chen, Y. S., and Cao, Q. J. Bifurcations and hysteresis of varying compliance vibrations in the primary parametric resonance for a ball bearing. *Journal of Sound and Vibration*, **350**, 171–184 (2015)

[9] Harris, T. A. and Mindel, M. H. Rolling element bearing dynamics. *Wear*, **23**, 311–337 (1973)

[10] Sunnersjö, C. S. Varying compliance vibrations of rolling bearing. *Journal of Sound and Vibration*, **58**, 363–373 (1978)

[11] Fukata, S., Gad, E. H., Kondou, T., Ayabe, T., and Tamura, H. On the radial vibrations of ball-bearing-computer-simulation. *Bulletin of JSME*, **28**, 899–904 (1985)

[12] Mevel, B. and Guyader, J. L. Routes to chaos in ball bearings. *Journal of Sound and Vibration*, **162**, 471–487 (1993)

[13] Mevel, B. and Guyader, J. L. Experiments on routes to chaos in ball bearings. *Journal of Sound and Vibration*, **318**, 549–564 (2008)

[14] Tiwari, T. and Gupta, K. Effect of radial internal clearance of a ball bearing on the dynamics of a balanced horizontal rotor. *Journal of Sound and Vibration*, **238**, 723–756 (2000)

[15] Tiwari, M., Gupta, K., and Prakash, O. Dynamic response of an unbalanced rotor supported on ball bearings. *Journal of Sound and Vibration*, **238**, 757–779 (2000)

[16] Harsha, S. P. Non-linear dynamic response of a balanced rotor supported on rolling element bearings. *Mechanical Systems and Signal Processing*, **19**, 551–578 (2005)

[17] Harsha, S. P. Nonlinear dynamic response of a balanced rotor supported by rolling element bearings due to radial internal clearance effect. *Mechanism and Machine Theory*, **41**, 688–706 (2006)

[18] Harsha, S. P. Nonlinear dynamic analysis of an unbalanced rotor supported by roller bearing. *Chaos Solitons and Fractals*, **26**, 47–66 (2005)

[19] Aktürk, N., Uneeb, M., and Gohar, R. The effects of number of balls and preload on vibrations associated with ball bearings. *ASME Journal of Tribology*, **119**, 747–753 (1997)

[20] Liew, A., Feng, N., and Hahn, E. Transient rotordynamic modeling of rolling element bearing systems. *ASME Journal of Engineering for Gas Turbines and Power*, **124**, 984–991 (2002)

[21] Jang, G. H. and Jeong, S. W. Nonlinear excitation model of ball bearing waviness in a rigid rotor supported by two or more ball bearings considering five degrees of freedom. *ASME Journal of Tribology*, **124**, 82–90 (2002)

[22] Jang, G. H. and Jeong, S. W. Analysis of a ball bearing with waviness considering the centrifugal force and gyroscopic moment of the ball. *ASME Journal of Tribology*, **125**, 487–498 (2003)

[23] Ghafari, S. H., Abdel-Rahman, E. M., Golnaraghi, F., and Ismail, F. Vibrations of balanced fault-free ball bearings. *Journal of Sound and Vibration*, **329**, 1332–1347 (2010)

[24] Bai, C. Q., Zhang, H. Y., and Xu, Q. Y. Subharmonic resonance of a symmetric ball bearing-rotor system. *International Journal of Non-Linear Mechanics*, **50**, 1–10 (2013)

[25] Zhang, X., Han, Q. K., Peng, Z. K., and Chu, F. L. Stability analysis of a rotor-bearing system with time-varying bearing stiffness due to finite number of balls and unbalanced force. *Journal of Sound and Vibration*, **332**, 6768–6784 (2013)

[26] Zhang, X., Han, Q. K., Peng, Z. K., and Chu, F. L. A comprehensive dynamic model to investigate the stability problems of the rotor-bearing system due to multiple excitations. *Mechanical Systems and Signal Processing*, **70-71**, 1171–1192 (2016)

[27] Gunduz, A. and Singh, R. Stiffness matrix formulation for double row angular contact ball bearings: analytical development and validation. *Journal of Sound and Vibration*, **332**, 5898–5916 (2013)

[28] Nonato, F. and Cavalca, K. L. An approach for including the stiffness and damping of elastohydrodynamic point contacts in deep groove ball bearing equilibrium models. *Journal of Sound and Vibration*, **333**, 6960–6978 (2014)

[29] Xu, L. X. and Li, Y. G. An approach for calculating the dynamic load of deep groove ball bearing joints in planar multibody systems. *Nonlinear Dynamics*, **70**, 2145–2161 (2012)

[30] Xu, L. X. A general method for impact dynamic analysis of a planar multi-body system with a rolling ball bearing joint. *Nonlinear Dynamics*, **78**, 857–879 (2014)

[31] Razpotnik, M., Bischof, T., and Boltežar, M. The influence of bearing stiffness on the vibration properties of statically overdetermined gearboxes. *Journal of Sound and Vibration*, **351**, 221–235 (2015)

[32] Hou, L., Chen, Y. S., Cao, Q. J., and Zhang, Z. Y. Turning maneuver caused response in an aircraft rotor-ball bearing system. *Nonlinear Dynamics*, **79**, 229–240 (2015)

[33] Zhao, C. J., Yu, X. K., Huang, Q. X., Ge, S. D., and Gao, X. Analysis on the load characteristics and coefficient of friction of angular contact ball bearing at high speed. *Tribology International*, **87**, 50–56 (2015)

[34] Jin, Y. L., Yang, R., Hou, L., Chen, Y. S., and Zhang, Z. Y. Experiments and numerical results for varying compliance vibrations in a rigid-rotor ball bearing system. *ASME Journal of Tribology*, **139**, 041103 (2017)

[35] Nayak, R. Contact vibrations. *Journal of Sound and Vibration*, **22**, 297–322 (1972)

[36] Hess, D. and Soom, A. Normal vibrations and friction under harmonic loads, part 1: Hertzian contact. *ASME Journal of Tribology*, **113**, 80–86 (1991)

[37] Rigaud, E. and Perret-Liaudet, J. Experiments and numerical results on non-linear vibrations of an impacting hertzian contact, part 1: harmonic excitation. *Journal of Sound and Vibration*, **265**, 289–307 (2003)

[38] Perret-Liaudet, J. and Rigaud, E. Response of an impacting Hertzian contact to an order-2 subharmonic excitation: theory and experiments. *Journal of Sound and Vibration*, **296**, 319–333 (2006)

[39] Fu, C. G. *Aeroengine Design Manual*, *Rotor Dynamics and Engine Body Vibration*, Vol. 19, Aviation Industry Press, Beijing (1999)

[40] Lazovic, T., Ristivojevic, M., and Mitrovic, R. Mathematical model of load distribution in rolling bearing. *FME Transactions*, **36**, 189–196 (2008)

[41] Marconnet, P., Pottier, B., Rasolofondraibe, L., Dron, J. P., and Kerroumi, S. Measuring load distribution on the outer raceways of rotating machines. *Mechanical Systems and Signal Processing*, **66-67**, 582–596 (2016)